CENTRIFUGAL FORMING AND MECHANICAL PROPERTIES OF SILICONE-BASED ELASTOMERS FOR SOFT ROBOTIC ACTUATORS

By

PARTH KULKARNI

A thesis submitted to the

Graduate School-New Brunswick

Rutgers, The State University of New Jersey

In partial fulfillment of the requirements

For the degree of

Master of Science

Graduate Program in Mechanical and Aerospace Engineering

Written under the direction of

Professor Aaron D. Mazzeo

And approved by

_____

_____

_____

_____

New Brunswick, New Jersey

October 2015

ABSTRACT OF THE THESIS

CENTRIFUGAL FORMING AND MECHANICAL PROPERTIES OF SILICONE-BASED ELASTOMERS FOR SOFT ROBOTIC ACTUATORS

By PARTH KULKARNI

Thesis Director:

Professor Aaron D. Mazzeo

This thesis describes the centrifugal forming and resulting mechanical properties of silicone-based elastomers for the manufacture of soft robotic actuators. This process is effective at removing bubbles that get entrapped within 3D-printed, enclosed molds. Conventional methods for rapid prototyping of soft robotic actuators to remove entrapped bubbles typically involve degassing under vacuum, with open-faced molds that limit the layout of formed parts to raised 2D geometries. As the functionality and complexity of soft robots increase, there is a need to mold complete 3D structures with controlled thicknesses or curvatures on multiples surfaces. In addition, characterization of the mechanical properties of common elastomers for these soft robots has lagged the development of new designs. As such, relationships between resulting material properties and processing parameters are virtually non-existent. One of the goals of this thesis is to provide guidelines and physical insights to relate the design, processing conditions, and resulting properties of soft robotic components to each other. Centrifugal forming with accelerations on the

order of 100 g’s is capable of forming bubble-free, true 3D components for soft robotic actuators, and resulting demonstrations in this work include an aquatic locomotor, soft gripper, and an actuator that straightens when pressurized. Finally, this work shows that the measured mechanical properties of 3D geometries fabricated within enclosed molds through centrifugal forming possess comparable mechanical properties to vacuumed materials formed from open-faced molds with raised 2D features.

ACKNOWLEDGEMENTS

I would like to thank my advisor, Professor Aaron D. Mazzeo for his support and guidance throughout the project. This project would not have been successful without his help. He is a great mentor and always encouraged me to push my limits. I thank him for giving me the wonderful opportunity to work on this project, and especially for his moral support during difficult times which I will always remember. I am also grateful to Professor Assimina A. Pelegri and Professor Hae Chang Gea for taking time out of their schedules and reviewing my thesis and providing me with their advice on the editing. All my lab mates have been of great help and provided tremendous support throughout my work. I would like to thank Jingjin Xie, Chen Yang, Yanjun Wang, Ke Yang, Xiangyu Gong, and John Popivchak for helping me out whenever I required any assistance in the lab. All of them made my time in the lab a lot of fun and made me look forward to come to the lab.

TABLE OF CONTENTS

LIST OF FIGURES

LIST OF TABLES

CHAPTER 1

INTRODUCTION

In the last few years, renewed interest in soft robotics has focused on creating machines with enhanced functionality. These soft robots made of compliant materials, such as polymers[1–4], elastomers, and hydrogels,[5,6] are capable of receiving power through pneumatic[1,4], chemical[7,8], or electrical means[9–12]. Pneumatically-driven soft robots are beginning to show promise in applications ranging from the manipulation of objects[2] to locomotion[4] to aerodynamics[14] to camouflage[3] to mechanical durability[15] to rehabilitation[16]. This work focuses on pneumatically-driven elastomeric soft actuators manufactured using platinum-cured Ecoflex (00-10, 00-30, and 00-50).

The state of art in the creation of soft robotic actuators, in many cases still relies on empirical experimentation and experience, and there are still opportunities to explore the manufacturing science associated with both centrifugal forming and general casting of elastomers. For casting of elastomers, there is a need to address issues with molding complete, complex, bubble-free, 3D structures with controlled thicknesses or curvatures for added functionality. The conventional methods for removing bubbles and forming silicone-based components in research labs typically involve degassing under vacuum. This process involves mixing the uncured polymer into a cup, pouring it in an open-faced mold, using a vacuum jar for degassing (it might also be necessary to remove the remaining bubbles manually after degassing with a vacuum jar[13]), and demolding. The study from Martinez et al.[2] demonstrated that vacuuming polydimethylsiloxane (PDMS) for 30 minutes and Ecoflex 00-30 for 5 minutes at 36 torr was capable of removing bubbles from

open-faced molds that limit the layout of molded components to raised 2D geometries. It is currently not possible to manufacture true 3D soft components using conventional open-faced molds. An enclosed mold is capable of producing the required geometries but using conventional techniques based on meso-scale soft lithography will not necessarily ensure the production of elastomeric components without entrapped bubbles.

Every forming process that converts material from a liquid state to that of a solid requires management or elimination of embedded bubbles. While 3D printers with elastomeric materials are beginning to demonstrate capabilities of printing soft materials[17], direct printing will continue to combat technical challenges associated with striation that can lead to permeability of pressurized gases or degradation in bulk mechanical properties, along with slow speeds of production. The soft 3D-printable materials of Ninjaflex and Tango Black have elastic moduli of 15.2 MPa and 0.3 MPa, respectively, while the currently commercially non-printable Ecoflex 00-30 has an elastic moduli of 0.092 MPa at a strain of 10% (see Figure 6). For these reasons, the preferred method of creating soft, tough elastomers still relies on casting.

The technique used in this paper solves the above problem with moderate gravity applied through centrifugal forming (Figure 1). This process makes it possible to fabricate parts free of bubble with geometries replicated from 3D printed molds. Centrifugal forming, as previously studied by Mazzeo et al.[18,19], is capable of removing bubbles in silicone-based microfluidic components. However, the cast microfluidic devices typically do not experience large strains or significant mechanical loading in operation. Thus, the emphasis was on removing bubbles for optical transparency instead of removing bubbles for mechanical properties. There is also a lack of processing rules relating the processing

conditions in centrifugal casting of components to resulting mechanical properties. To simulate and design the behavior of complex geometries, we need to know the stress-strain behavior of the material, and this behavior is dependent on processing conditions[20,21].

This paper provides a tool for researchers and innovators to design and fabricate new, unique soft robotic actuators which might not be possible with conventional methods using vacuum-based degassing. Mechanical testing and associated constitutive models will enable finite element-based simulation of elastomeric actuators[20,22]. Enabling the simple production of 3D geometries will enable faster iterations through designs and new actuators. The technique outlined in this work should also be compatible with materials besides standard silicone-based elastomers, such as hydrogels, epoxies, and low-melt metals.

Figure 1:

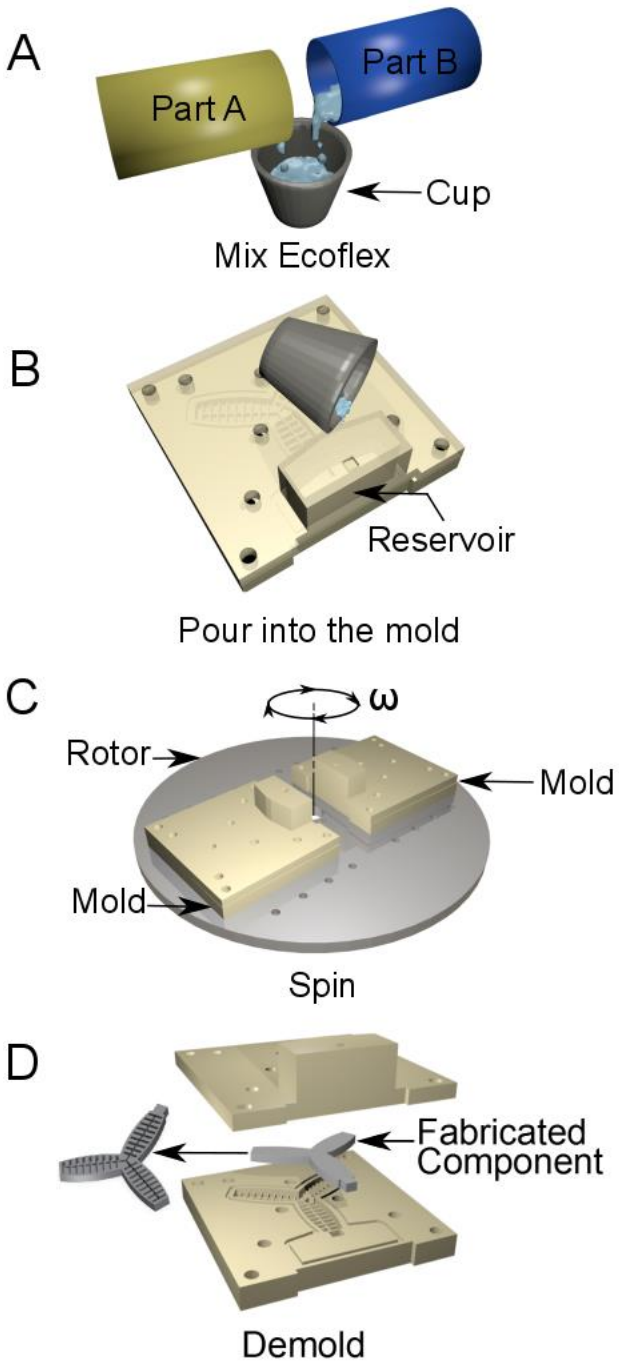

Figure 1: Process for fabrication of a soft component. (a) Mixing of Ecoflex part A and part B in a container. (b) Transferring the mixed polymer into the reservoir of the mold. (c) Spinning the mold in the centrifuge at a specified time and speed. (d) Demolding the cured component.

CHAPTER 2

EXPERIMENTAL DESIGN

2.1 Centrifugal Forming with 3D-printed and Laser-ablated Molds

We designed the molds in a computer-aided-design (CAD) software (SolidWorks) and used a 3D printer (Stratasys uPrint SE, and Flashforge) to manufacture low-cost molds for forming as described in this article. The features in the 3D-printed molds were inverse geometries of those molded. A portion of the mold near the axis of rotation contained a reservoir to hold the Ecoflex in its uncured, liquid form (See SI for more information). A laser (VersaLaser) cut Poly(methyl methacrylate) (PMMA) to fabricate transparent faces of the molds for real-time observation of moving bubbles during spinning and stationary curing.

Centrifugal casting/forming is a proven method to manufacture components from a variety of materials such as metals, polymers, and thermoplastics. As shown by Mazzeo et al., this method can be used for rapid-prototyping of silicone components[18]. Centrifugal forming is also suitable for rapid-prototyping of bubble-free soft actuators with true 3D shapes. We used two centrifuges in this work, one with a fixed, steady-state rotational speed (Jouan RC 10-10) and one with controllable rotational speed and swinging buckets (Jouan CR-412). The Jouan RC 10-10 centrifuge spins at 1100 rpm, which corresponded to accelerations ranging from 34 g's to 168 g's, depending on the position within the mold relative to the axis of rotation. For the customized rotor, the maximum dimensions of the mold that can be accommodated is 120 mm x 120 mm (Figure 2). The Jouan CR-412 centrifuge has a variable rotational speed ranging from 150 rpm to 2000 rpm. The

maximum dimension of the mold that can fit in the centrifuge is 100 mm x 150 mm.

Various studies related to centrifugal forming have shown that two physical phenomena occur during spinning. The removal of bubbles depends on the balance of two mechanisms: buoyant forcing of the bubbles from the bulk of the liquid to an exit near the axis of rotation at a liquid-air interface[23,24] and dissolution based on a gradient in concentration of dissolved air in the wall of the bubbles and the surrounding liquid[24–28]. Both of these phenomena occur simultaneously during spinning. Previous studies showed that there is a specific or critical size of a bubble which requires the maximum time to be removed from the solution, by a combination of buoyant force and mass transfer of gas through the wall of the bubble. The physical behavior (buoyant transport or mass transfer) which dominates the removal of bubbles depends on its size relative to the critical size. Buoyancy dominates the bubble removal process above the critical size and diffusion dominates below the critical size.

2.2 Mechanical Testing of Centrifugally Formed Samples

2.2.1 Design of Specimens

We used a dumbbell-shaped specimen to perform tensile tests (Figure 3(a) and (b)). The test section of the dumbbell-shaped specimen has a width of 4 mm, a thickness of 2 mm, and a length of 35 mm. The overall length is 64 mm and the width of gripping section is 12.5 mm. The dimensions of the dumbbell-shaped sample are such that it breaks in the narrow test section during the tensile test. It is important to use appropriate radius of curvature (between gripping section and test section), length of the test section and smooth surfaces on molds to avoid failure during tensile testing due to stress concentration.

2.2.2 Fabrication of the Specimens

We prepared the uncured prepolymer of Ecoflex 00-10, 00-30, and 00-50 for the test specimen by measuring and mixing Part A and Part B in a ratio of 1:1 by mass. The manufacturer recommends mixing Part B of Ecoflex thoroughly before mixing it with part A of Ecoflex. We closed the mold with the help of fasteners and inserted it inside the bucket of the centrifuge. We then prepared all the samples by manually stirring the precursors in a disposable cup for 2 minutes with a craft stick and inserted the mixture into the reservoir of the mold with the help of a syringe. We spun the centrifuge for the duration as mentioned in the Table 1. The varied spinning times for samples ranged from 2 minutes to 15 minutes with speeds imposing local gravity on the order of 10 g's. We selected duration of spinning, such that with each increasing time period, there was a reduction in number of visible bubbles in the test samples. The last time of duration listed in each cell for spin times within the table represents the processing condition in which there were no visible bubbles left in the sample. For each set of processing conditions, we prepared and mechanically tested five samples.

2.2.3 Curing/Cross-linking

After spinning, we let the thermosets in the mold cure at room temperature for 4 hours (3 hours for Ecoflex 50). We also let the samples post-cure for 2 hours at 80 ºC and 1 hour at 100 ºC before demolding the samples.

2.2.4 Tensile Testing of the Samples

An Instron-4411 with a load cell of 500 N (maximum capacity) provided mechanical displacement and measured the force. We attached the wider ends of the test specimen between the pneumatic grips of the tensile testing machine. The narrow region of the sample formed the test section. We used a position-controlled method to test the samples. In this method the machine pulled the specimen at a constant rate of displacement of 30 mm/min and the load cell measured the resulting force at a sampling rate of 1 Hz. To determine the strain and strain rate during the material testing, the specimens had reflective fiducial markers on each end of the test region of the stretched sample. We placed the camera in front of the fiducial markers to take the images at 1 frame per second (fps). A 5.0-Megapixel camera from Point Grey (Model no. GRAS-50S5M-C), Sony (HDR CX760V) and Nikon D7100 served as a video extensometer with the tracking of fiducial marks processed with the MATLAB Image Processing Toolbox.

2.3 Examples of Functioning Soft Robotic Actuators

To fabricate different types of soft actuators, we prepared the Ecoflex as described and poured it into the reservoir of the mold. We spun the mold for the soft gripper (SI Figure 4) in the Jouan CR-412 for 15 minutes at 800 rpm, with local gravity of 105 g's acting at the centroid of the mold (143 mm from the axis of rotation). The time for spinning the mold for the jellyfish-like soft robot (Figure 4) in the Jouan RC-1010 was also 15 minutes with a rotational speed of 1100 rpm, resulting in a local gravity of 108 g's at a distance of 80 mm from the axis of rotation.

The inverse soft mechanism shown in this work is a pre-curved actuator bent in two separate directions, which becomes straight when powered pneumatically. This

straightening with positive pressure is in contrast to bending, which is the behavior commonly associated with the inflation of pneumatic soft actuators[1,2,4]. To make the inverse soft actuator, we spun the mold for 1100 rpm for 15 minutes in the Jouan CR-412. This component demonstrated a complex 3D actuator that can be manufactured by centrifugal forming method.

Figure 2:

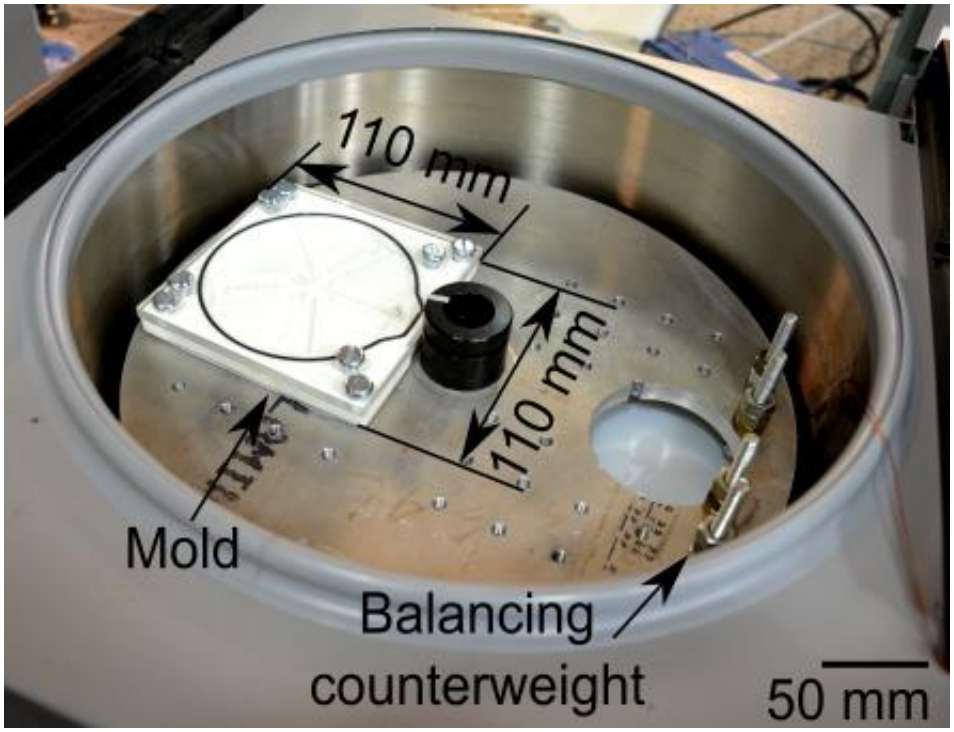

Figure 2: Jouan RC 10-10 centrifuge with a custom rotor to accommodate molds ranging from 25 x 25 mm to 120 x 120 mm. To minimize vibration, a set of counterweights or an additional mold balances the spinning rotor.

Figure 3:

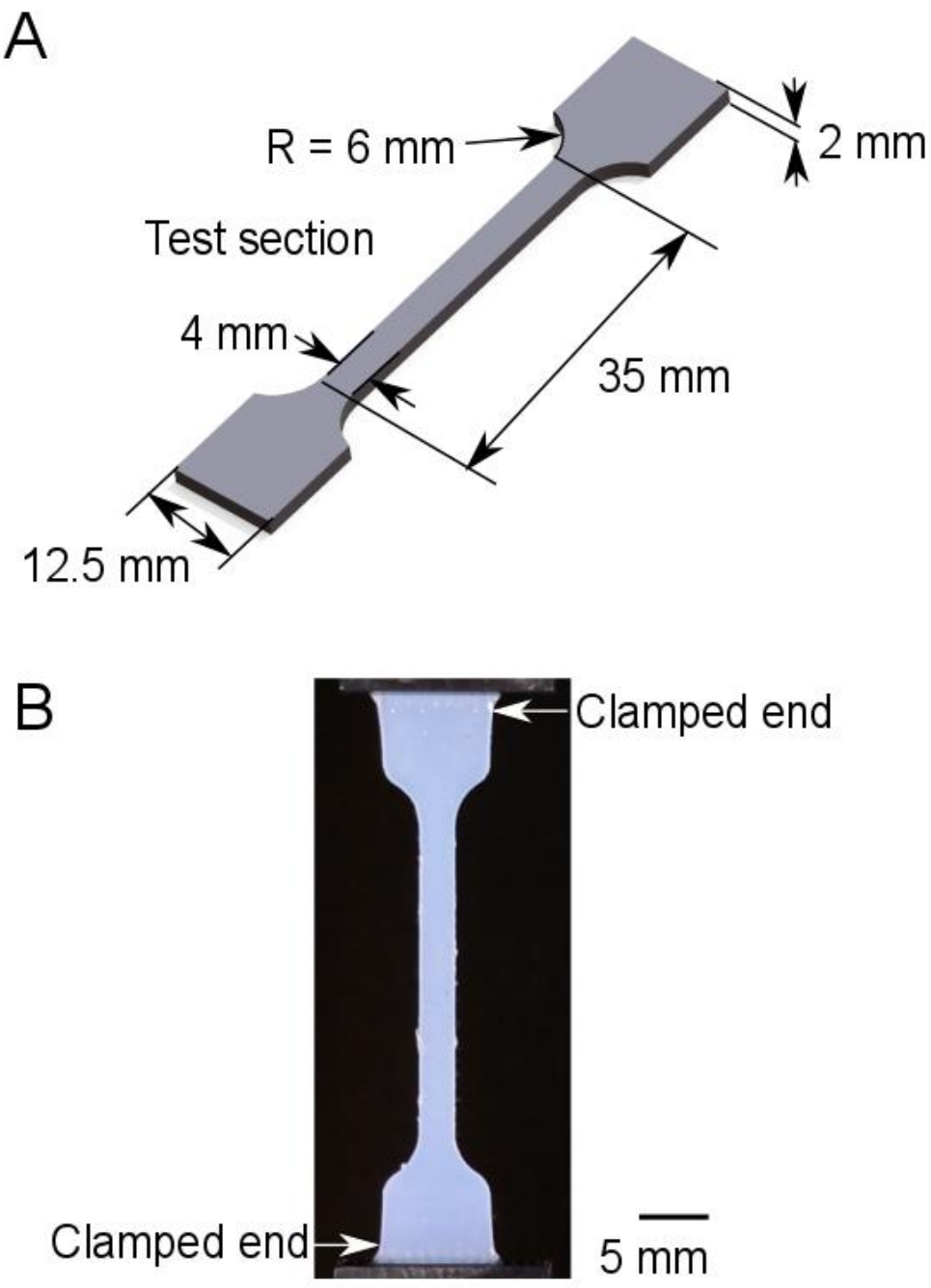

Figure 3: (a) The designed test sample with its dimensions. (b) The molded sample after spinning it in the centrifuge. The sample is clamped in the fixture of a tensile testing machine.

Table 1: The processing conditions used for fabricating the tensile test samples. The columns show the process parameter for Ecoflex 00-10, 00-30, and 00-50.

Material	**Spin Speed (RPM)**	**Acceleration (g)**	**Spin Time (minutes)**	**Viscosity (centiPoise)**	**Curing time (hours)**
Ecoflex 00-10	500±10	41.6	2, 3, 4, 14	14000	4 (room temp) + 2 (80 ºC) + 1 (100 ºC)
Ecoflex 00-30	350±10	20.4	1, 3, 4, 12	3000	4 (room temp) + 2 (80 ºC) + 1 (100 ºC)
Ecoflex 00-50	450±10	33.7	1, 3, 4, 15	8000	3 (room temp) + 2 (80 ºC) + 1 (100 ºC)

CHAPTER 3

RESULTS AND DISCUSSION

3.1 Effect of Centrifugation on the Mechanical Properties

The results from tensile testing of bubble-free samples by conventional processing with a vacuum jar and centrifugal forming showed that centrifugal forming produced parts with mechanical properties similar to those produced in a vacuum jar. From Figure 5, we can see that the ranges of ±1 standard deviation of the spun samples and conventional samples overlap each other, which suggests that material responses are not statistically distinct from each other. Figure 5 also shows that the stress-strain averages of each set of spun samples and conventional samples vary from each other. We observed this behavior for all three materials tested in the Ecoflex series (00-10, 00-30, and 00-50). The averages of the spun samples have higher moduli than the samples made from conventional processing. These changes in moduli might be due to the entrapment of dissolved air, which affects the cross-linking or distribution of nanoscopic concentrations of stress.

3.2 Effect of Bubbles on the Mechanical Properties

Next, we performed tensile tests on samples spun in a centrifuge for time less than that required to remove all bubbles. The results showed that the entrapped bubbles alter the mechanical properties of the samples (Figure 6). Bubbles caused the test samples to break at lower stresses and strains. For Ecoflex 00-30 the samples with bubbles broke at 30%-40% lower stress. These changes in mechanical properties might have detrimental effects on formed soft actuators, as localized strains might equal 500%. While there are arguably

some changes in the effective moduli of the materials at strains greater than 100%, the most pronounced effects of entrapped bubbles are on the ultimate tensile strength or breaking of the material samples. We also observed variations in the mechanical properties between the five test samples for each case (Figure 5 and Figure 6). These variations were significantly higher for strains greater than 200%. These deviations may have resulted from small changes in processing conditions, such as changes in ambient temperature during curing or localized heating during post-curing which might have affected the cross-linking of the polymer. It can also be due to intrinsic variation in the material itself with respect to distributions of molecular weight. The work by Schneider et al. also showed similar variations in mechanical properties of RTV 615 and Sylgard 184[29]. The data from Figure 6 showed that the ±1 standard deviation of the samples with bubbles (spin duration of 1 min-4min) overlapped each other, and they are therefore likely not statistically distinct from each other. We also observed that the averages of samples with bubbles have a higher elastic moduli compared to the samples with no bubbles, especially at strains greater than 200% until ultimate failure. These changes in moduli at higher strains are likely due to changes of the effective areas in the narrow test sections of the samples caused by entrapped bubbles. The entrapped bubbles are visible in Figure 7.

3.3 Growth of Bubbles during Curing/Polymerization

From our experiments, we noticed that some samples appeared free of bubbles after spinning with visual inspection, but the bubbles grew during curing of the samples. The increases in the sizes of the bubbles and appearance of new bubbles from microscopic bubbles/ seeds observed results from diffusion (Figure 8). This growth (or shrinkage) is

dependent on the difference between the concentration of air inside the wall of the bubble and the concentration of air in the surrounding polymer (Ecoflex)[19,30]. If the concentration of air inside the wall of the bubble is less than the concentration of air in the surrounding polymer, the bubble will grow as a result of diffusion of air into the bubble from the surrounding polymer. If the concentration of air inside the wall of the bubble is more than the concentration of air in the surrounding polymer, the bubble will shrink. In our case, the concentration of air inside the wall of the bubble appeared to be less than the concentration of air in the surrounding liquid, as the bubbles tended to grow in size.

3.4 Simulations and Demonstrations of Soft Robotic Actuators

Figure 9 shows the stress-strain plots for Ecoflex 00-10, 00-30, 00-50, along with the fitted material models. The measured mechanical properties are suitable for simulations, as shown in Figure 10 and SI Figure 6. We have used a five-term Mooney-Rivlin material model for Ecoflex 00-10 and a reduced polynomial model (Yeoh) for Ecoflex 00-30 and Ecoflex 00-50.

The five-term Mooney-Rivlin model[31,32] is defined by the following strain energy potential.

$$\cup = C_{10}(I_1 - 3) + C_{01}(I_2 - 3) + C_{20}(I_1 - 3)^2 + C_{02}(I_2 - 3)^2 + C_{11}(I_1 - 3)(I_2 - 3)$$

where U is the is the strain energy per unit of reference volume,C_{10},C_{01},C_{20},C_{02}, and C_{11} are the coefficients of the polynomial, and I_1, and I_2 are the stress invariants.

The Yeoh model[33] is defined by the following strain energy potential.

$$\cup = C_{10}(I_1 - 3) + C_{20}(I_1 - 3)^2 + C_{30}(I_1 - 3)^3$$

where U is the is the strain energy per unit of reference volume, C_{10}, C_{20}, and C_{30} are the coefficients of the polynomial, and $I_1$is the stress invariant. The coefficients for Ecoflex 00-10, 00-30, and 00-50 are given in Table 2.

Figure 10 shows the inverse soft actuator along with a simulation a performed in COMSOL Multiphysics. The inverse actuator was manufactured using uncured prepolymer, 3D printed molds, and a centrifuge as described in experimental design. The demonstrated component takes advantage of the new process. The actuator has curvatures in three directions, in that the 3D geometry of the actuator (without the strain-limiting layer) is formed in one simple step without entrapped bubbles. The conventional process would require the actuator to be fabricated in 2 or 3 separate steps. Figure 10(a) shows the simulation obtained with the help of stress-strain data.

Figure 11 shows a jellyfish-like soft robot that can move underwater. It has five actuators which acts as fins. The actuators bend when they are powered (inflated) and propel the jellyfish forward. While the channels are compatible with both air and water, we powered (inflated) the device pneumatically for fast inflation and deflation with the low viscosity of air. Figure 11(b) and (c) show the distance covered by the jellyfish-like soft robot in 9 and 18 seconds.

Figure 4:

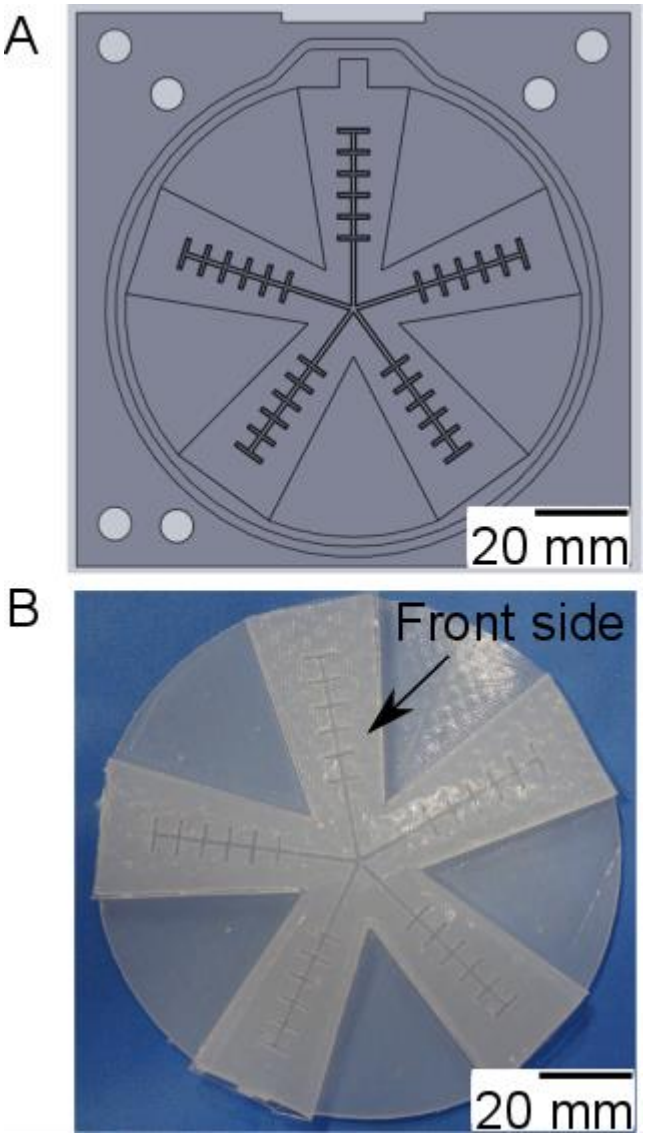

Figure 4: Fabrication of a jellyfish-like actuator (a) CAD-based mold for the jellyfish (b) An image of the manufactured jellyfish by spinning it in the centrifuge for 15 minutes at 1100 rpm. The front side of jellyfish is attached to a strain-limiting layer of PDMS.

Figure 5:

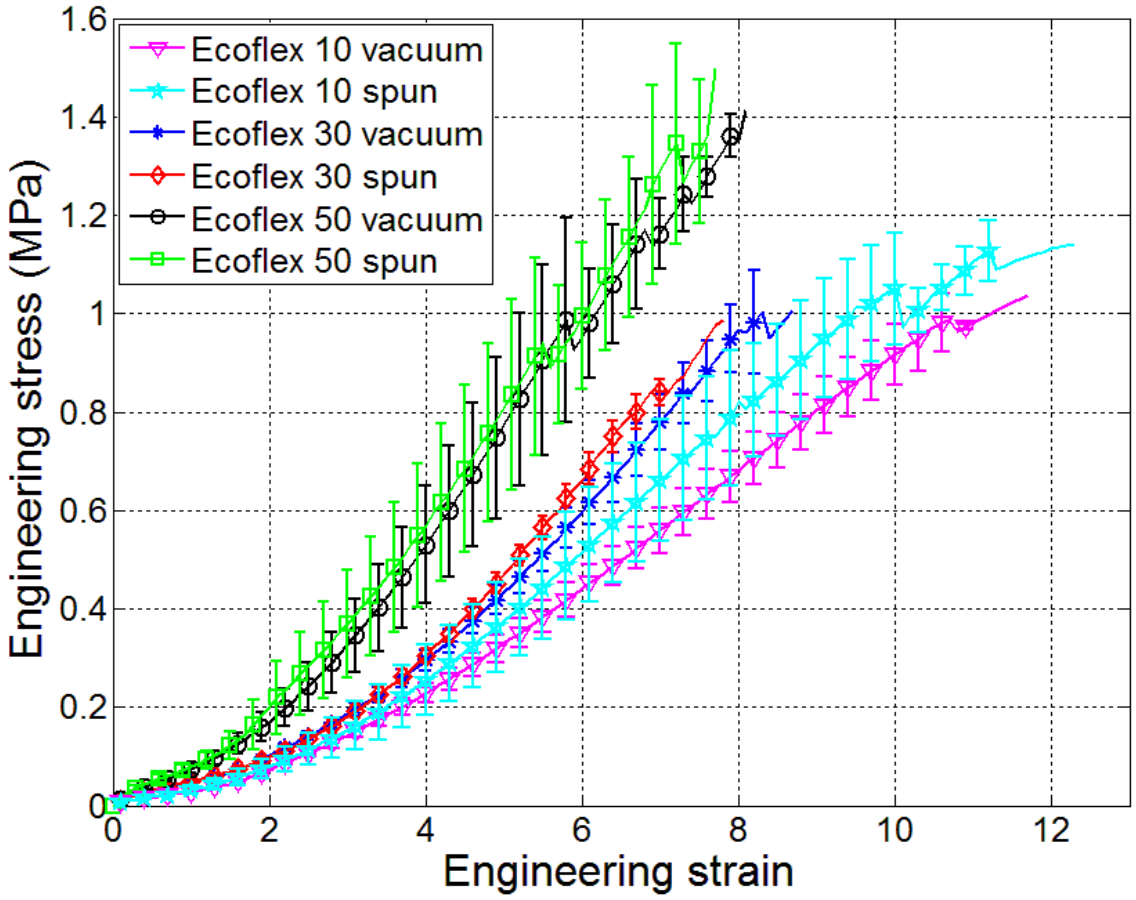

Figure 5: Results from tensile testing of samples prepared using a vacuum jar and centrifugal forming (spun). The plotted results are averages of five distinct samples for each condition with the error bars being ±1 standard deviation. The jagged nature in the lines comes from the failure of different samples.

Figure 6:

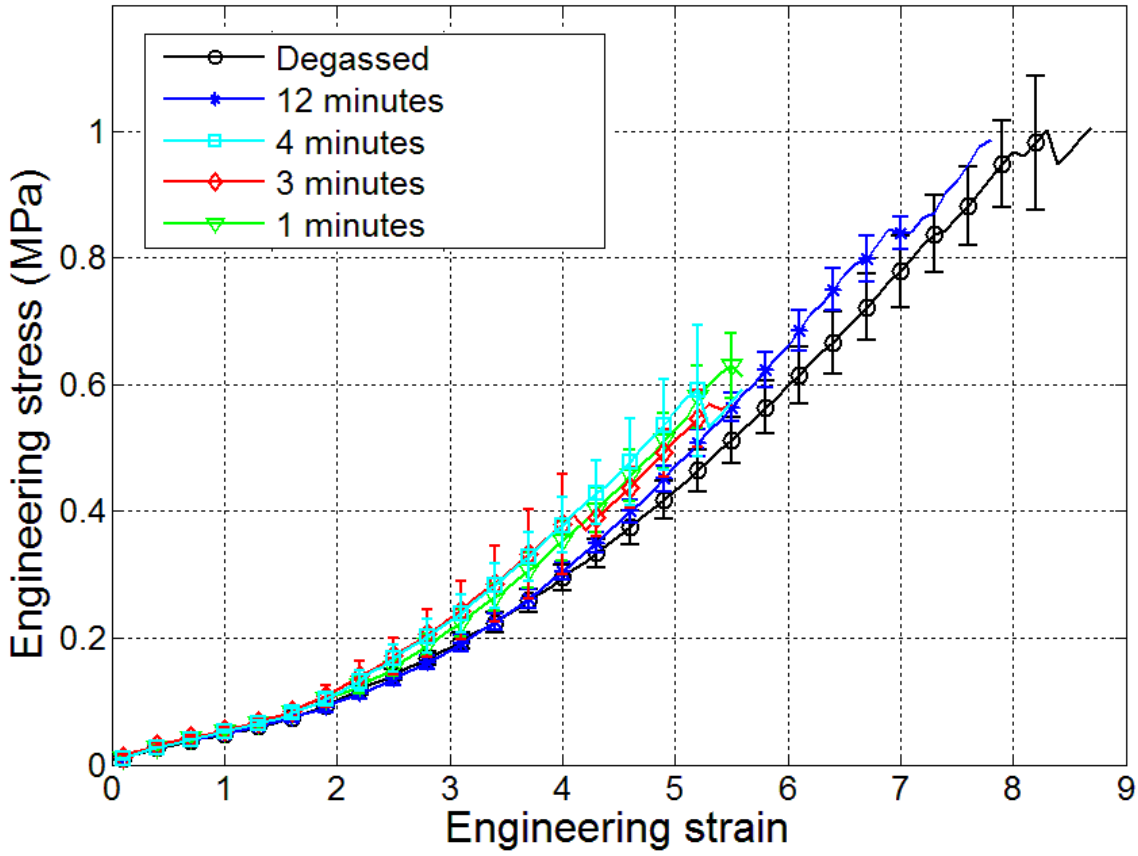

Figure 6: The plot shows the mechanical stress-strain response of Ecoflex 00-30 spun for various periods of time as described in Table 1. The samples spun for 1 min, 3 min, and 4 min had bubbles entrapped in them. The samples with bubbles broke at lower stresses and strains, and they have a slightly higher modulus than the samples with no bubbles. The plotted results are averages of five distinct samples for each condition with the error bars being ±1 standard deviation

Figure 7:

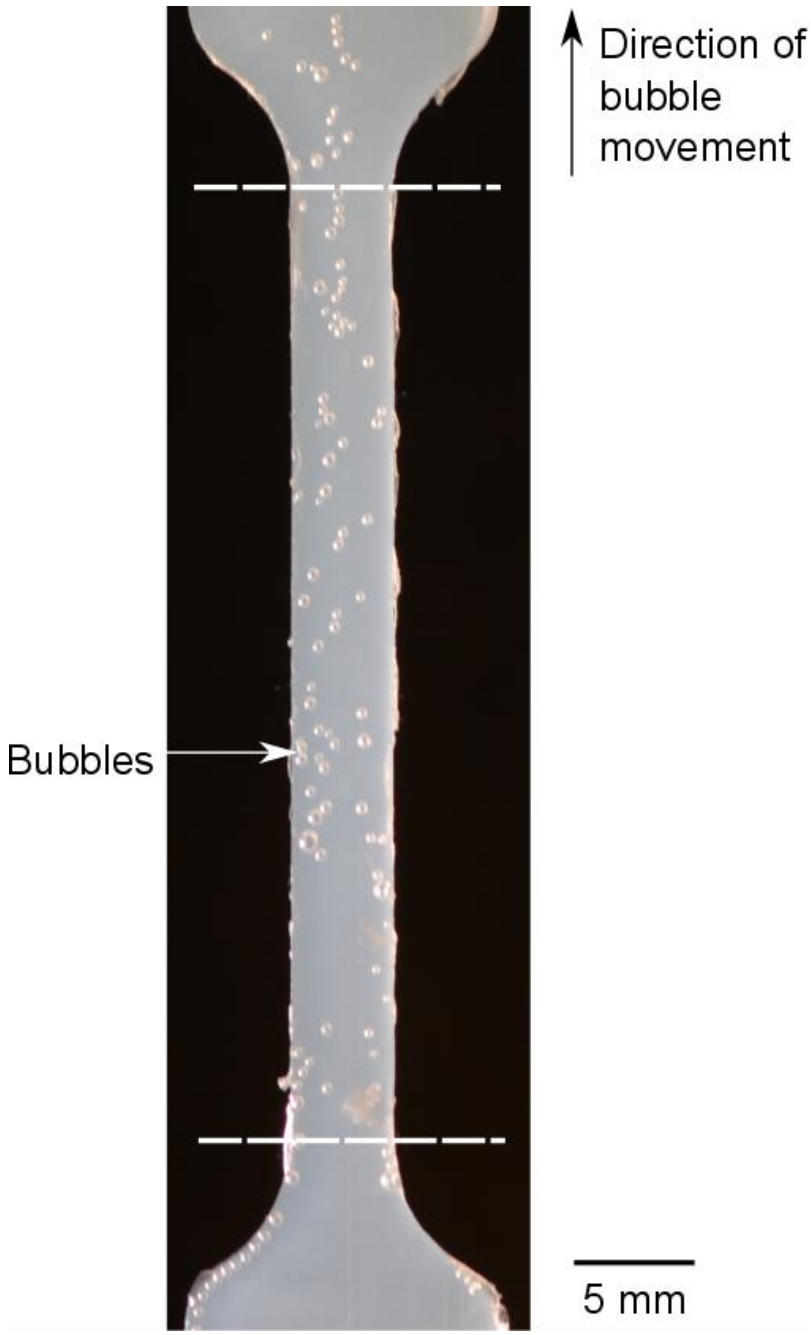

Figure 7: A test sample (Ecoflex 00-30) spun for 1 minute at 350±10 RPM. In this case the spin time was not sufficient to remove all the bubbles from the sample. The bubbles are visible throughout the central test section (region between the dashed lines).

Figure 8:

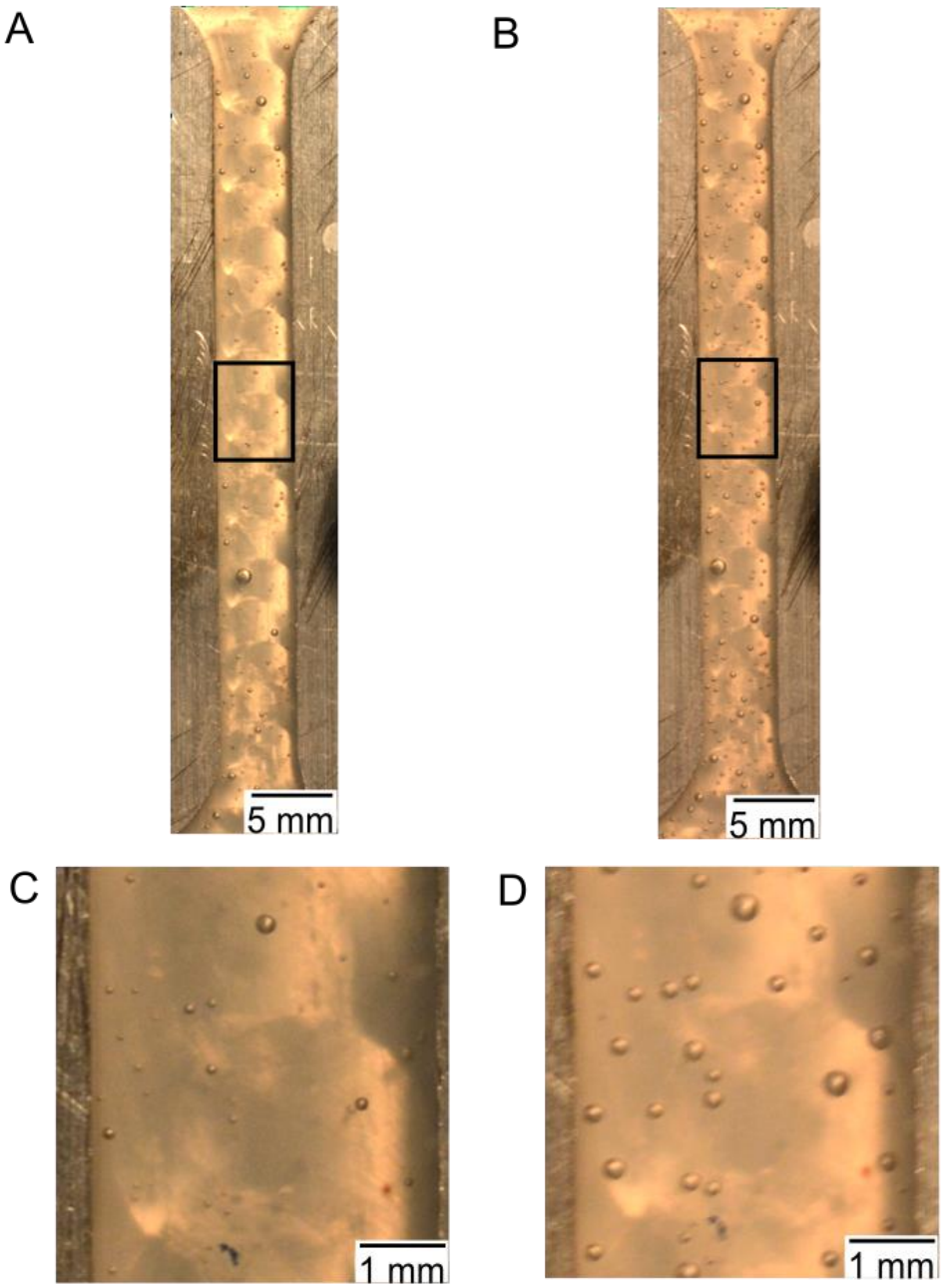

Figure 8: Images of bubbles entrapped in Ecoflex 00-30 spun for 1 minute in an uncured and cured state. (a) This image shows the bubbles at the start of the curing process. (b) View of the complete sample at the end of curing process (at room temperature). (c) Close-up section of Figure A. (d) Close-up section of Figure B.

Figure 9:

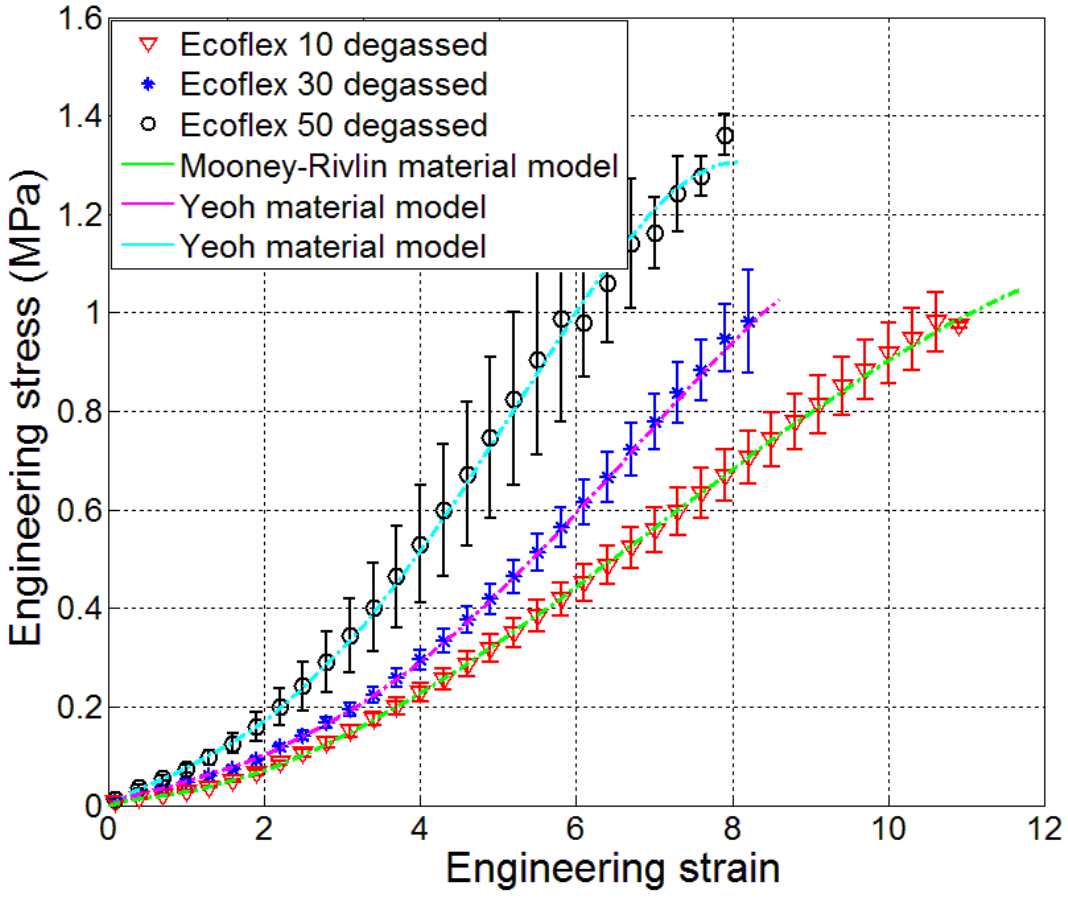

Figure 9: The plot shows degassed Ecoflex 00-10, 00-30 and 00-50 and the material models.

Figure 10:

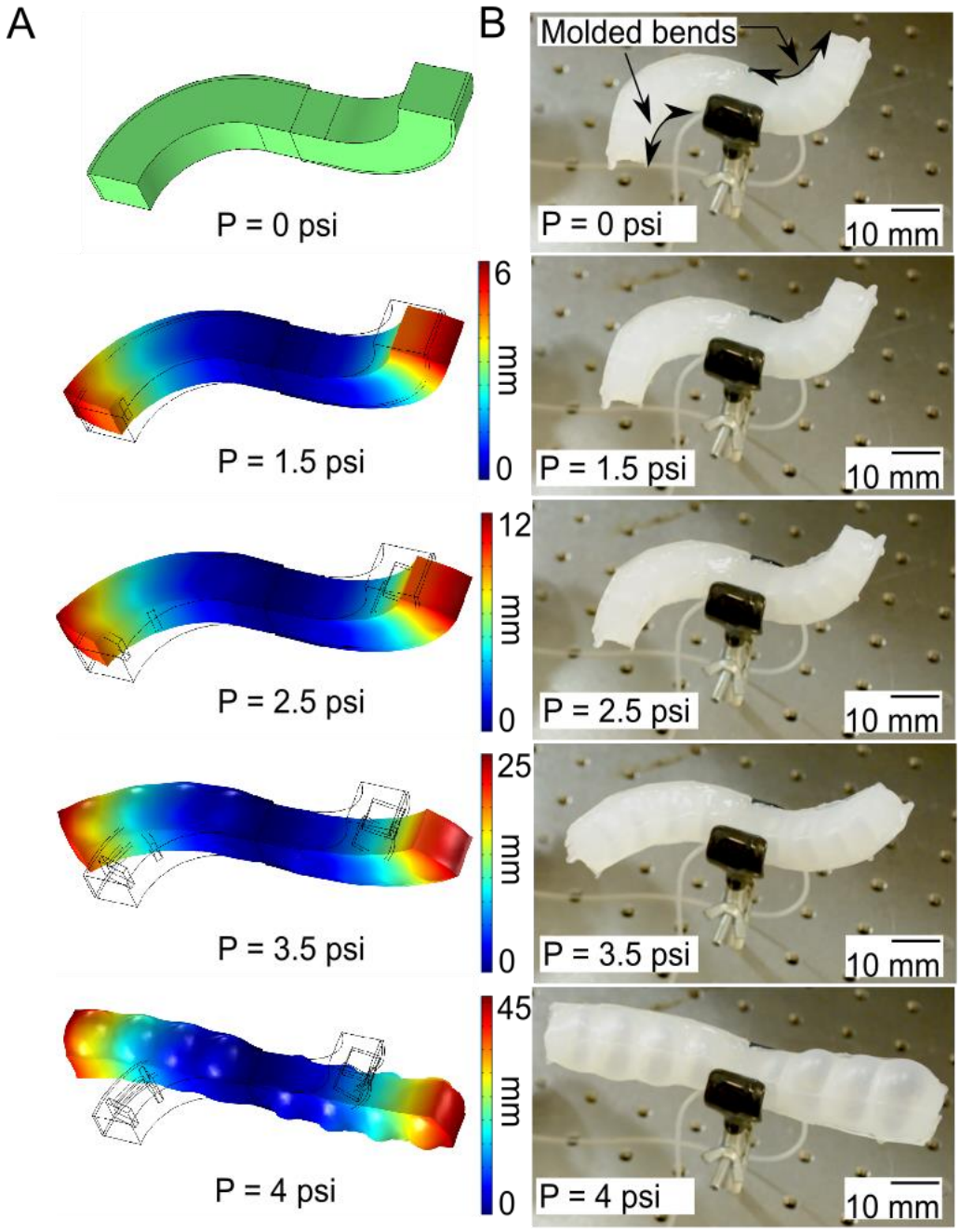

Figure 10: Comparasion between the response obtained by simulation and the fabricated inverse actuator. (a) Simulated behaviour of the inverse soft robot as a fuction of pressure. (b) Inverse actuator manufactured by spinning at 1100 rpm for 15 minutes. The images show the actuator being inflated at various pressures.

Figure 11:

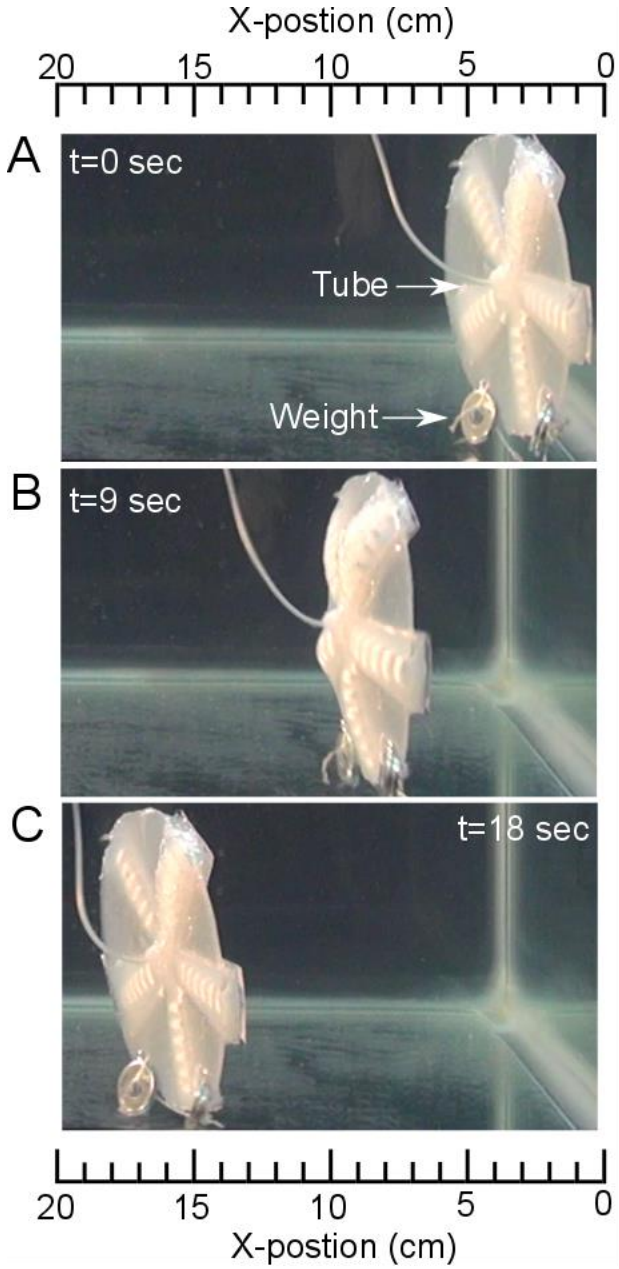

Figure 11: Jellyfish-like soft robot moving under water. (a) The initial position of the jellyfish. The weights shown in the picture are to counterbalance the effect of buoyancy. (b) The image shows the location of the jellyfish at t =9 seconds. (c) The image shows the location of the jellyfish at t =18 seconds. It covers a distance of 13 cm from the initial position. See SI Video for more details.

CHAPTER 4

CONCLUSIONS

We investigated centrifugal forming as a low-cost method to fabricate three-dimensional (3D) components from silicone-based elastomers of current importance to the production of actuators for soft robots. Centrifugal forming with moderate accelerations is capable of removing entrapped bubbles of gas to produce test samples and complex 3D soft robotic actuators (soft gripper, aquatic robot, and inverse mechanism) with mechanical properties comparable to those produced by conventional degassing. It is also shown that spinning for shorter periods of time (<15 minutes) at these modest accelerations results in the entrapment of bubbles, which alters the mechanical properties of molded components. Since many of the research labs are already equipped with centrifuges making this process low cost, defect-free and conducive to rapid prototyping.

In addition, characterization of the mechanical properties of common elastomers for these soft robots has lagged the advancement of new designs. Measured stress-strain data for completely cured Ecoflex 00-10, 00-30 and 00-50 will enable designers to model and simulate responses of actuators before building them. It is also possible to use this method to manufacture small quantities of components per day.

Table 2: Coefficients of the fitted material models for Ecoflex series.

Material and Material Model	**Ecoflex 00-10 Five-term Mooney-Rivlin (MPa)**	**Ecoflex 00-30 Yeoh (MPa)**	**Ecoflex 00-50 Yeoh (MPa)**
Coefficients	C_{10} = -7.48 x 10^{-3} C_{01} = 1.96 x 10^{-2} C_{20} = -1.98 x 10^{-4} C_{02} = -5.39 x 10^{-4} C_{11} = 3.21 x 10^{-3}	C_{10} = 1.27 x 10^{-2} C_{20} = 4.23 x 10^{-4} C_{30} = -1.45 x 10^{-6}	C_{10} = 1.9 x 10^{-2} C_{20} = 9 x 10^{-4} C_{30} = -4.75 x 10^{-6}

References

1. Ilievski, F., Mazzeo, A. D., Shepherd, R. F., Chen, X. & Whitesides, G. M. Soft robotics for chemists. *Angew. Chem.* **123,** 1930–1935 (2011).
2. Martinez, R. V. *et al.* Robotic Tentacles with Three-Dimensional Mobility Based on Flexible Elastomers. *Adv. Mater.* **25,** 205–212 (2013).
3. Morin, S. A. *et al.* Camouflage and Display for Soft Machines. *Science* **337,** 828–832 (2012).
4. Shepherd, R. F. *et al.* Multigait soft robot. *Proc. Natl. Acad. Sci.* **108,** 20400–20403 (2011).
5. Lee, H., Xia, C. & Fang, N. X. First jump of microgel; actuation speed enhancement by elastic instability. *Soft Matter* **6,** 4342–4345 (2010).
6. Otake, M., Kagami, Y., Inaba, M. & Inoue, H. Motion design of a starfish-shaped gel robot made of electro-active polymer gel. *Robot. Auton. Syst.* **40,** 185–191 (2002).
7. Shepherd, R. F. *et al.* Using Explosions to Power a Soft Robot. *Angew. Chem. Int. Ed.* **52,** 2892–2896 (2013).
8. Palleau, E., Morales, D., Dickey, M. D. & Velev, O. D. Reversible patterning and actuation of hydrogels by electrically assisted ionoprinting. *Nat. Commun.* **4,** (2013).
9. Stokes, A. A., Shepherd, R. F., Morin, S. A., Ilievski, F. & Whitesides, G. M. A Hybrid Combining Hard and Soft Robots. *Soft Robot.* **1,** 70–74 (2013).
10. Lin, H.-T., Leisk, G. G. & Trimmer, B. GoQBot: a caterpillar-inspired soft-bodied rolling robot. *Bioinspir. Biomim.* **6,** 026007 (2011).
11. Carpi, F., Bauer, S. & De Rossi, D. Stretching dielectric elastomer performance. *Science* **330,** 1759–1761 (2010).

12. Keplinger, C., Kaltenbrunner, M., Arnold, N. & Bauer, S. Röntgen's electrode-free elastomer actuators without electromechanical pull-in instability. *Proc. Natl. Acad. Sci.* **107,** 4505–4510 (2010).
13. Mosadegh, B. *Soft Robotics Toolkit*. at <http://softroboticstoolkit.com/book/pneunets-step-2>
14. Xie, J. *et al.* Elastomeric Actuators on Airfoils for Aerodynamic Control of Lift and Drag. *Adv. Eng. Mater.* (In Press).
15. Tolley, M. T. *et al.* A Resilient, Untethered Soft Robot. *Soft Robot.* **1,** 213–223 (2014).
16. Polygerinos, P. *et al.* Towards a soft pneumatic glove for hand rehabilitation. in *2013 IEEE/RSJ International Conference on Intelligent Robots and Systems (IROS)* 1512–1517 (2013). doi:10.1109/IROS.2013.6696549
17. Richard, C. blossom. *Blossom* at <http://www.richardclarkson.com/blossom/>
18. Mazzeo, A. D. & Hardt, D. E. Centrifugal Casting of Microfluidic Components With PDMS. *J. Micro Nano-Manuf.* **1,** 021001–021001 (2013).
19. Mazzeo, A. D., Lustrino, M. E. & Hardt, D. E. Bubble removal in centrifugal casting: Combined effects of buoyancy and diffusion. *Polym. Eng. Sci.* **52,** 80–90 (2012).
20. Mosadegh, B. *et al.* Pneumatic Networks for Soft Robotics that Actuate Rapidly. *Adv. Funct. Mater.* **24,** 2163–2170 (2014).
21. Case, J. C., White, E. L. & Kramer, R. K. Soft Material Characterization for Robotic Applications. *Soft Robot.* **2,** 80–87 (2015).
22. Soft Robotics Toolkit. at <http://softroboticstoolkit.com/home>
23. Spencer, C. D. Centrifugal Casting of Thermoplastics. *Soc. Plast. Eng. - J.* **18,** 774–

779 (1962).

24. Sheard, E. A. Removing bubbles from castable liquid polyurethane raw materials. *Elastomerics* **122,** 49–55 (1990).
25. Spence, A. G. & Crawford, R. J. Removal of Pinholes and Bubbles from Rotationally Moulded Products. *Proc. Inst. Mech. Eng. Part B J. Eng. Manuf.* **210,** 521–533 (1996).
26. Kontopoulou, M. & Vlachopoulos, J. Bubble dissolution in molten polymers and its role in rotational molding. *Polym. Eng. Sci.* **39,** 1189–1198 (1999).
27. Crawford, R. J. *Rotational molding technology*. (Plastics Design Library/William Andrew Pub, 2002).
28. Gogos, G. Bubble removal in rotational molding. *Polym. Eng. Sci.* **44,** 388–394 (2004).
29. Schneider, F., Fellner, T., Wilde, J. & Wallrabe, U. Mechanical properties of silicones for MEMS. *J. Micromechanics Microengineering* **18,** 065008 (2008).
30. Epstein, P. S. & Plesset, M. S. On the Stability of Gas Bubbles in Liquid-Gas Solutions. *J. Chem. Phys.* **18,** 1505–1509 (1950).
31. Mooney, M. A Theory of Large Elastic Deformation. *J. Appl. Phys.* **11,** 582–592 (1940).
32. Rivlin, R. S. Large Elastic Deformations of Isotropic Materials. IV. Further Developments of the General Theory. *Philos. Trans. R. Soc. Lond. Math. Phys. Eng. Sci.* **241,** 379–397 (1948).
33. Yeoh, O. H. Some Forms of the Strain Energy Function for Rubber. *Rubber Chem. Technol.* **66,** 754–771 (1993).

CHAPTER 5

APPENDIX

5.1 Custom Rotor and Holder for the Centrifuge

We designed and manufactured a custom rotor (SI Figure 2) for centrifuge Jouan RC 10-10 and a holder for Jouan RC-412 (SI Figure 1). This modification allowed us to use molds of different dimensions in the centrifuge. We retrofitted centrifuge Jouan RC-412 with a custom heater having higher temperature range than the inbuilt heater. With this modification it is possible to heat the centrifuge up to 100 ºC while spinning. Although we did not use this in our experiments, it can be used for future work.

5.2 Molds for tensile testing

The molds were made from multipurpose Aluminum alloy 6061 (SI Figure 3). We decided to machine cut the molds instead of using 3D printed molds because of the smoother surface finish associated with metal cutting. A rough or striated surface of the molded samples can cause stress concentrations at the edges. The molds were machined using a 1/8 inch end mill on a 3-axis CNC machine.

5.3 Sealing of the mold

Sealing is one of the important thing to consider when designing the mold to avoid the leakage of the material while spinning. It necessary to have a sealing mechanism for molds experiencing a gravity of 50 g’s or more. The material itself can act as a sealant for

molds experiencing low forces of gravity (<50 g's). In our design, we sealed the mold with the help of an O-ring of 2 mm diameter (SI Figure 4(A)). We machined a groove of 1.8 mm height and 2 mm width around the main design to fit the O-ring.

5.4 Reservoir Sizing

Reservoir is a small container at the top side of the mold to hold the liquid prepolymer. The ideal size of the reservoir is equal to the volume of the cast components, but due to size constraints it is not always possible to design a full-size reservoir. In our experiments, we found that the reservoir with half the volume of cast components can still be enough since the liquid prepolymer fills some part of the mold during initial fill-up of the reservoir.

5.5 Tensile Testing

The image below (SI Figure 5) shows a casted test sample attached to a tensile testing machine. We made sure that the tensile test sample is in an exact vertical position as possible to avoid uneven stress distribution in the sample. A camera tracks the reflective type fiducial markers attached to the central section of the sample. We manually activated the Instron tensile testing machine and camera simultaneously. The mismatch between start time for the camera and measured forces is in microseconds. Since we used slow speed of extension (30 mm/min) the mismatch between the tensile testing machine and camera is insignificant. The strains were calculated using a MATLAB image processing code given at the end.

SI Figure 1

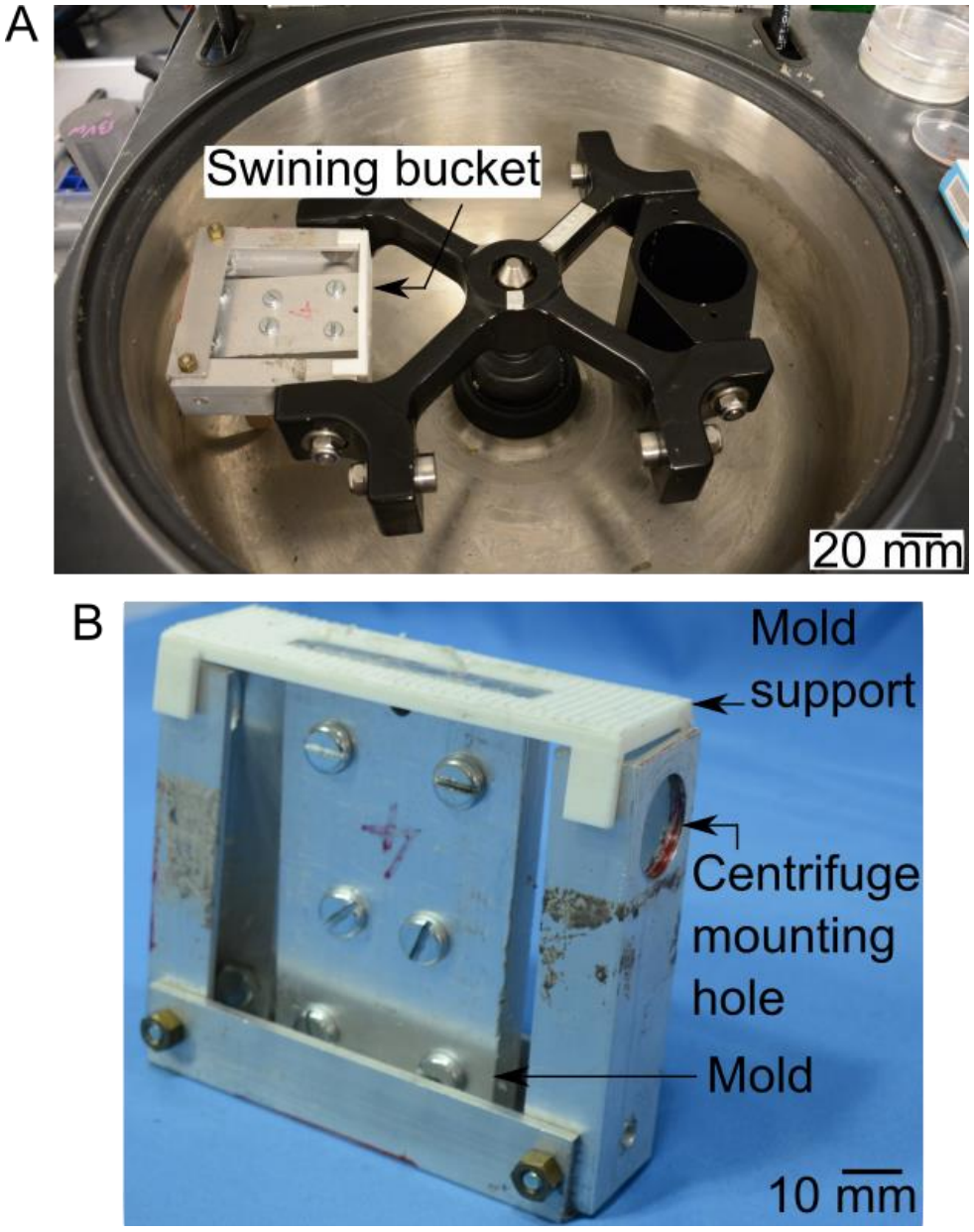

SI Figure 1: (a) The figure shows a Jouan CR-412 centrifuge with a custom holder made from Aluminum alloy. The shown position of the Aluminum holder is same as it would be during spinning. The bucket with the black color is the original holder of the centrifuge. (b) A detailed view of custom holder with an inserted mold for the swinging bucket centrifuge.

SI Figure 2

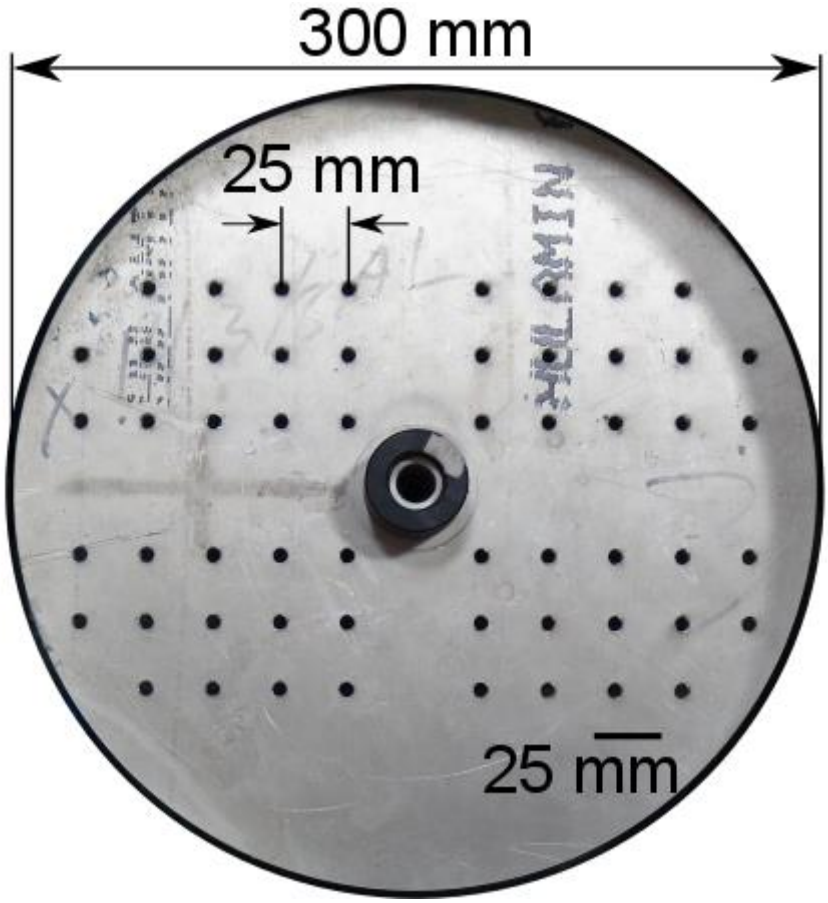

SI Figure 2: A custom rotor made from Aluminum Alloy 6061 for Jouan RC-1010. There are 56-1/4 inch threaded holes in the rotor to accommodate molds of different shapes and sizes. The threaded holes makes it easy to attach and remove the molds.

SI Figure 3

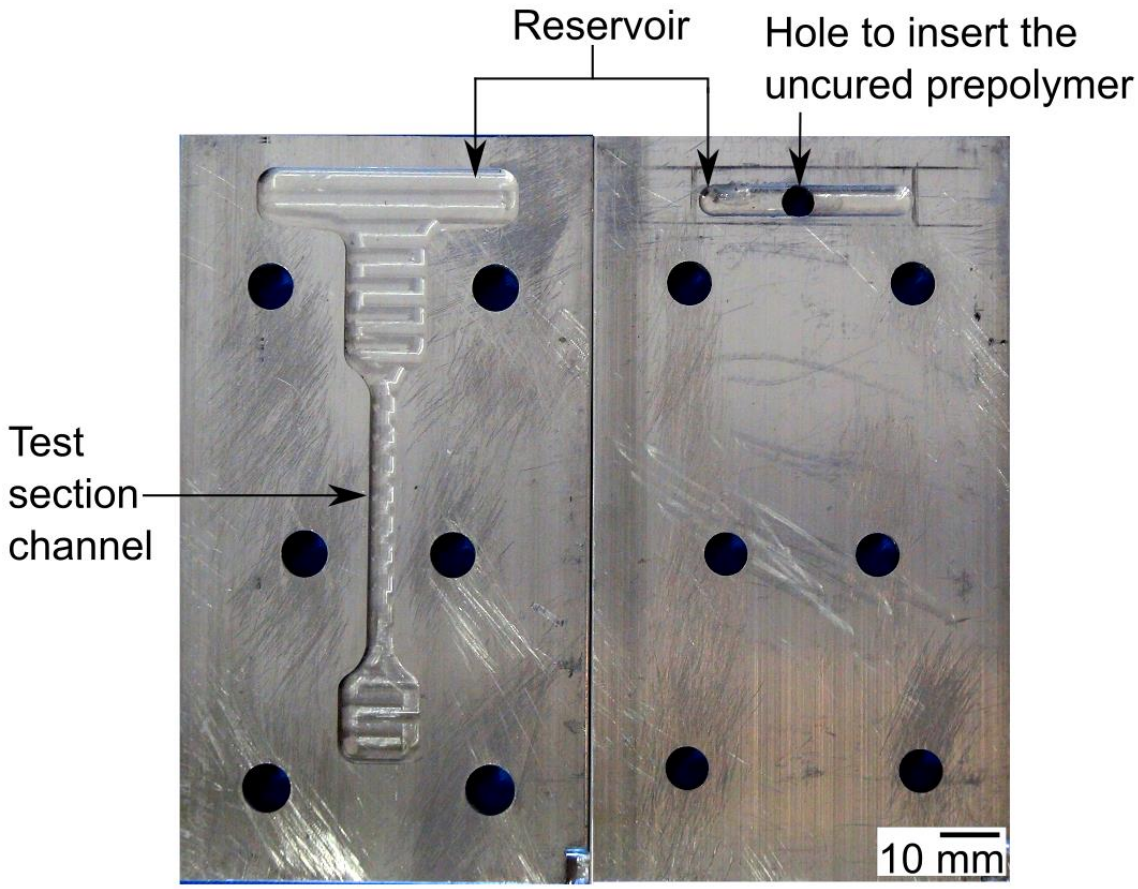

SI Figure 3: An aluminum mold used for fabricating dogbone samples by centrifugal forming. The reservoir at the top side of the mold is used to store liquid polymer before spinning. The 6 holes shown in the image are for fastening the mold.

SI Figure 4

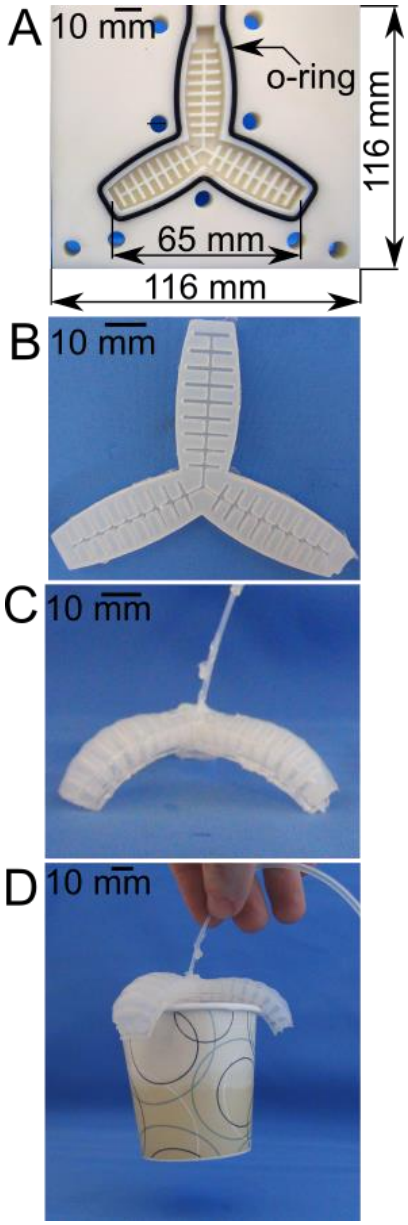

SI Figure 4: Image of a soft gripper. (a) A 3D-printed mold for fabricating the gripper. An O-ring is used around the main design for sealing purpose. (b) A cast soft gripper made from Ecoflex 00-30. (c) The image shows the soft gripper in an actuated state. The arms of the gripper bend inwards when they are inflated. (d) The gripper can hold and lift small objects. The image shows the gripper lifting a paper cup.

5.6 Simulation of the Soft Robotic Actuators

We used the commercially available software COMSOL Multiphysics to simulate the behavior of the soft robotic actuators. First, we performed the analysis on 3D model of dumbbell-shaped sample for the three Ecoflex series and compared the results with the actual testing to check for accuracy of the simulation. We built the 3D models using Solidworks and used the Time-Dependent study of the Solid Mechanics module for the analysis. We imported the Solidworks model in COMSOL as a Solidworks file or stl file. The meshing is done using the automatic meshing algorithm provided by COMSOL. We kept the mesh size as 'fine' to generate elements. In Time-Dependent study, the force/pressure is applied as a function of time. Since the simulation is highly non-linear, it is important to keep the force/pressure applied per step to be small. The dumbbell-shaped sample is modelled as Yeoh hyperelastic material model for Ecoflex 00-30 and 00-50, and as Mooney-Rivlin model for Ecoflex 00-10. The coefficients for the material models are given in Table 2. After assigning the material, we applied a total force of 7 N on the dumbbell-shaped model. The force-displacement results are shown in SI Figure 6.

To simulate the inverse actuator, we follow similar steps as above. We imported the model in COMSOL as a Solidworks assembly file. The inverse actuator is made of the extensible actuator (Ecoflex) and the inextensible layer (Sylgard 184). We modeled the inextensible layer as linear elastic with a Young's Modulus of 3 MPa and Poisson's ratio of 0.49 and the extensible actuator as a hyperelastic model (Yeoh). To see the response of the inverse actuator under inflation, we applied a pressure of 4 psi on the pneumatic channels of the actuator. Comparative results with the simulated model and actual model are shown in Figure 10.

SI Figure 5

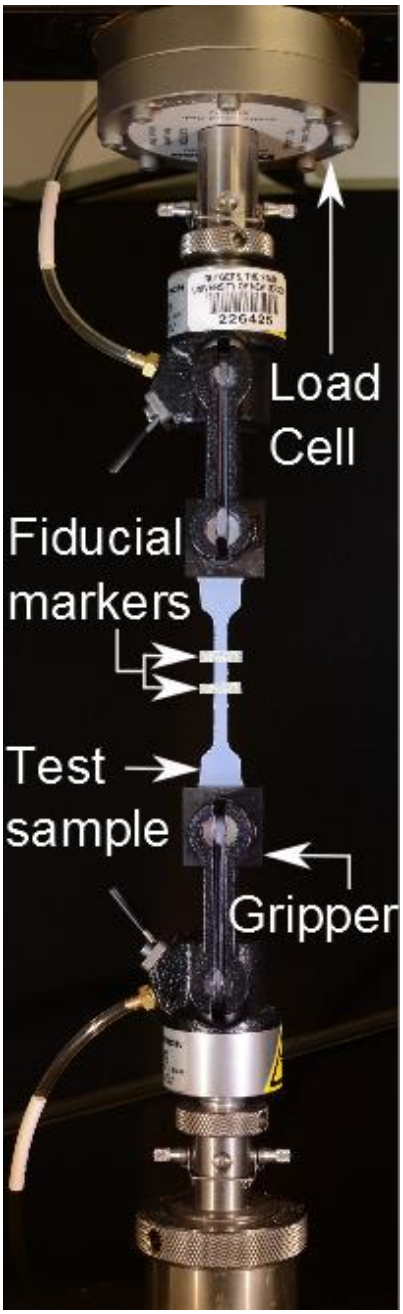

SI Figure 5: Sample mounted on a tensile testing machine (Instron-4411) with the fiducial markers on it. We use image processing to calculate the strains by tracking the fiducial markers.

SI Figure 6

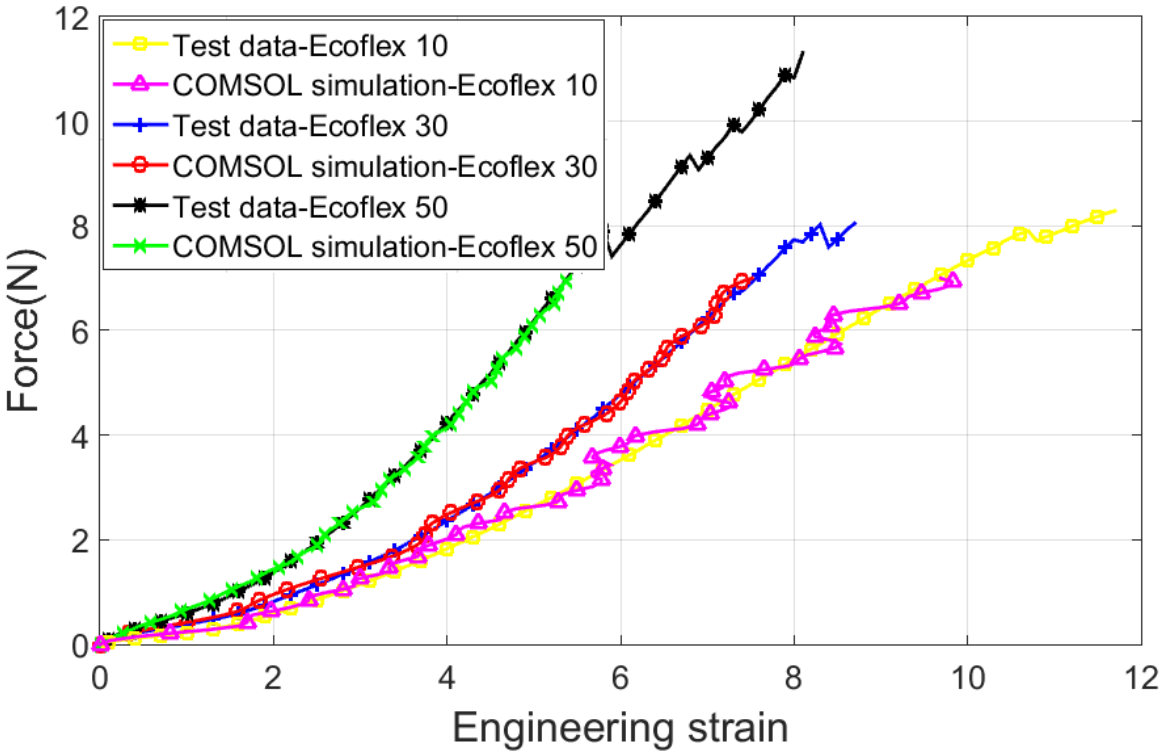

SI Figure 6: Verification of uniaxial tensile test data from simulation and experimentation for Ecoflex series. The simulation data is obtained by applying a force of 7N to a dumbbell-shaped 3D model. The jagged nature of curve for Ecoflex 10 simulation data is due to remeshing of the finite element model during the processing.